IOP Conf. Series: Materials Science and Engineering **256** (2017) 012010 doi:10.1088/1757-899X/256/1/012010

Peculiarities of living cell response to the external stimuli revealed via quasistatic mode of atomic force microscopy

M M Khalisov[1,2,*], A V Ankudinov[2,3], V A Penniyaynen[1], T E Timoshenko[1], K I Timoshchuk[2], M V Samsonov[4] and V P Shirinsky[4]

[1] Pavlov Institute of Physiology RAS, Saint Petersburg, 199034, Russia
[2] ITMO University, Saint Petersburg, 197101, Russia
[3] Ioffe Institute, Saint Petersburg, 194021, Russia
[4] National Cardiology Medical Research Center, Moscow, 121552, Russia

[*]hamax@list.ru

Abstract. The technique of atomic force microscopy allows revealing living cell morphology and mechanical properties characterization under physiologically relevant conditions. Here, we review our recent results on living cell reaction to different external influences obtained by this technique. The Bruker PeakForce QNM quasistatic mode was used to study living fibroblasts, erythrocytes, sensory neurons, and endothelial cells.

1. Introduction

In the last decades, atomic force microscopy (AFM) has become one of the common tools in cell biology research. Now AFM is widely used for living animal cell characterization [1, 2]. This imaging method allows studying cell morphology and mechanical properties with submicrometer resolution and under physiologically relevant conditions.

Various cellular processes are associated with mechanical properties of cells: shape maintenance, migration, differentiation, and division [3]. Several pathologies are known to change the cell mechanical phenotype [4]. Although the living cells are not perfectly elastic objects, in AFM studies their mechanical properties are mostly described by Young's modulus. The measurement of the Young's modulus of a single cell is based on the AFM nanoindentation technique. It implies that the AFM probe compresses the sample with a preset force, and the induced cell deformation is employed to calculate the Young's modulus according to the selected contact mechanics model [3].

AFM Force Spectroscopy and Force Volume are the most widespread modes for living cell Young's modulus measurements. These modes are slow in operation and have low data flow rate. Recently developed quasistatic AFM modes, such as PeakForce QNM (Bruker), are much faster; therefore, they appear to be promising for living cell examination. PeakForce QNM and other similar modes force the AFM tip oscillate well below its resonance frequency and press against the sample surface for a short period of time. The manner of operation enables simultaneous topography and mechanical properties data acquisition. Since PeakForce QNM mode was integrated into commercial AFM systems not long ago, the information on its application to living cells is pretty scarce [5-7]. We utilized AFM in PeakForce QNM mode to study the mechanical properties of different types of living cells. The aim of this work was to examine and analyze the specifics of AFM investigation of living chicken embryo cardiac fibroblasts, rat erythrocytes, chicken embryo sensory neurons, and mouse microvascular endothelial cells under physiologically relevant conditions.

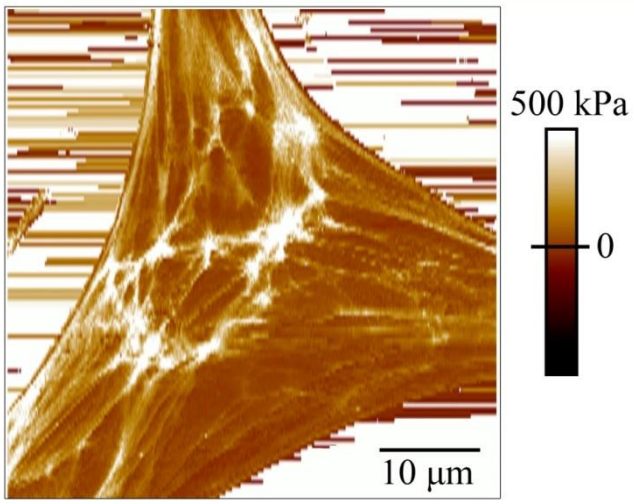

Figure 1. AFM map of Young's modulus of living cardiac fibroblast obtained using a sharp tip. The AFM imaging parameters: peak force – 3 nN, probing amplitude and vertical frequency – 1.0 μm and 250 Hz, horizontal scanning frequency – 0.1 Hz.

2. Materials and methods

All experiments were performed using the atomic force microscope (Bruker BioScope Catalyst) combined with the inverted optical microscope (Carl Zeiss Axio Observer). During the AFM imaging in PeakForce QNM mode, the cells were in physiological solution at 37ºC. AFM data were processed in NanoScope Analysis 1.50 and Gwyddion 2.44.

We studied cardiac fibroblasts of 10-12-day-old chicken embryos using two types of AFM probes: conventional sharp tips ($R \leq 12$ nm) and colloidal indenters ($R = 325$ nm) [8]. The information on the sample handling is found in [9].

3. Results and discussion

As expected, sharp probes enabled more detailed AFM images. As a consequence, Young's modulus maps permitted single cytoskeletal filaments identification in the submembrane layer of cell (Fig. 1).

The apparent Young's moduli of fibroblast determined using Sneddon (sharp tips) and Hertz (colloidal probes) models differed considerably: $E_{Sneddon}/E_{Hertz} \approx 5$. At the same time, the mean of cell maximum height and the contact stiffness were similar when using sharp as well as submicron spherical indenters: ≈ 1.7 μm and ≈ 18 mN/m, respectively. The result of our observations implies that, in PeakForce QNM AFM, Young's modulus is inaccurate to quantify fibroblast mechanical properties; contact stiffness is preferable instead. Since the fibroblast contact stiffness did not depend on the AFM tip shape, we suppose that the external cell layer behaves as a hard shell and its deformation is determined only by the applied load.

The next object studied is a living erythrocyte or red blood cell. Extreme deformability of living erythrocytes prevents their effective AFM testing. Therefore, these cells are often examined in the hardened fixed state. In practice, such a state is attained by erythrocyte chemical treatment or drying, but fixing precludes analysis of cell native elastic properties, which are of great interest. In order to overcome this limitation, living erythrocytes are immobilized on adhesive substrate polylysine. A few examples of AFM investigations of living red blood cells on polylysine may be found in [10–13]. Yet polylysine was reported to be able to modify erythrocyte properties and even to invoke lysis. The authors [14] stated that erythrocyte deposition on polylysine led to the shift of cell shape to a spherical cap following by the plasma membrane damage due to the sustained static membrane tension. Optical observation indeed confirmed these conclusions: over time living erythrocytes "vanished".

We imaged living rat erythrocytes attached to polylysine in PeakForce QNM mode of AFM. Sample preparation procedure is presented in [15]. Using optical microscope, we also detected disappearance of some cells with the passage of time. However, in contrast to Hategan et al. [14], our findings show that erythrocytes do not actually vanish; instead, they change their optical contrast and shape as well as rigidity. Firstly, after the deposition red blood cells spread on the polylysine substrate.

In this case, the cells are flat and highly deformable. Besides, they possess optical contrast relative to the adhesive layer. Subsequently, erythrocytes swell, becoming convex and stiff. Moreover, the cells simultaneously lose their color when monitoring in the optical microscope. That is, as decolorized erythrocytes are visualized via AFM, we conclude that they maintain their integrity during the discovered transformation. In one AFM experiment, we have managed to visualize the erythrocyte transformation process (Fig. 2).

We have shown that living erythrocytes tend to transform on the polylysine substrate. The erythrocyte state characterized by cell swelling and hardening precedes lysis. In general, our findings indicate that the plasma membrane extra tension induced by cell-substrate strong adhesion should be taken in consideration while performing living cell AFM studies.

AFM was also employed to study the living sensory neuron response to substances with analgesic effect. Comenic acid (CA) was shown to relieve chronic pain [16]. This chemical has become an active ingredient of the novel non-opioid painkiller "Anoceptin" [17]. Another promising substance for analgesia is ouabain in nanomolar concentration, which is capable to decrease the voltage sensitivity of sensory neuron slow sodium $Na_v1.8$ channels responsible for pain signals in mammals [18, 19]. We used AFM to clarify, if CA and ouabain affect the morphology and elastic properties of living sensory neurons.

The AFM sample preparation protocol one can find in [20]. Dorsal root ganglia neurons of 10-12-day chicken embryos were cultivated on polylysine in the presence of CA (10^{-8} M) or ouabain (10^{-10} M). Using AFM we investigated the morphology and Young's modulus of living neurons of three groups: control cells, CA- and ouabain-treated neurons.

No morphology changes were detected in living sensory neurons under the influence of CA and ouabain. The control and CA-treated neurons manifested close mean Young's modulus values: 115 ± 90 kPa (n = 30) and 120 ± 97 kPa (n = 21), respectively. However, the mean neuron Young's modulus of cells after ouabain treatment was somewhat higher: 172 ± 109 kPa (n = 15). Although the ouabain-treated sensory neuron elasticity surpassed the control cell elasticity by a factor of approximately 1.5, Mann-Whitney U-test showed no statistically significant difference between two Young's modulus values ($p = 0.08$).

Interestingly, earlier we observed the similar effect of ouabain on sensory neurons cultivated on collagen-fibronectin-coated Petri dishes [21]. The same trend of neuron stiffening after ouabain treatment on two diverse substrate types verifies the consistency of our results. The fact, that ouabain stiffens sensory neurons and CA does not, testifies to the substances activate signaling pathways that differ from each other.

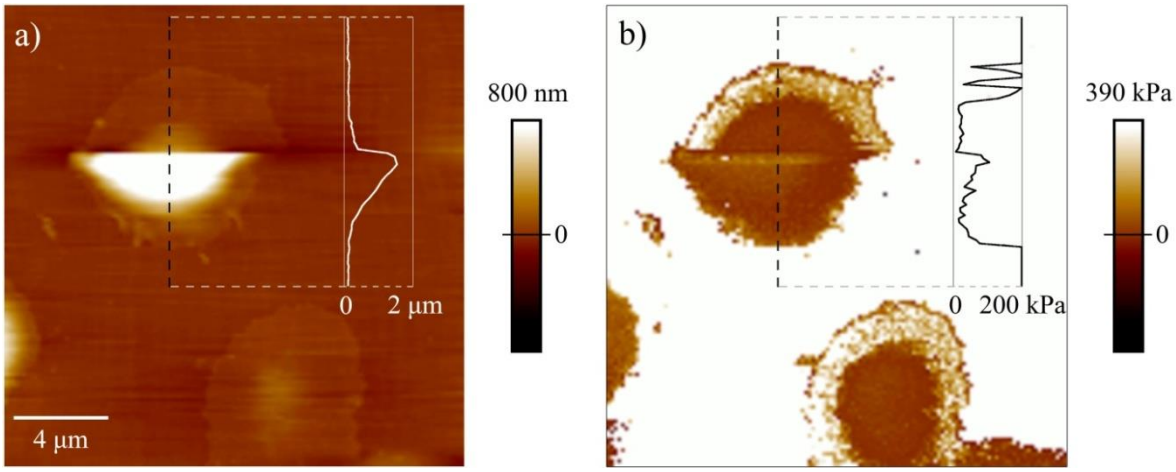

Figure 2. AFM (a) topography and (b) Young's modulus map of living rat erythrocytes. AFM imaging parameters: peak force 0.5 nN; probing amplitude and vertical frequency 1.0 µm and 250 Hz; horizontal scanning frequency 0.1 Hz; slow scan direction – from top to bottom.

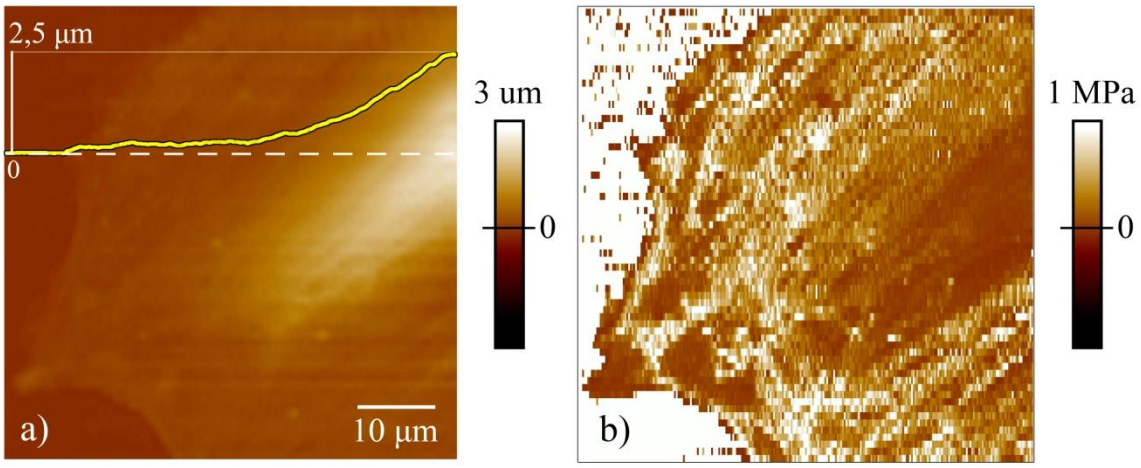

Figure 3. AFM EC (a) height image and (b) Young's modulus map. AFM imaging parameters: peak force 1 nN; probing amplitude and vertical frequency 0.5 μm and 250 Hz; horizontal scanning frequency 0.15 Hz.

AFM PeakForce QNM millisecond indentation thus allows tracing changes in Young's modulus of sensory neuron values in response to addition of chemical agents with analgesic effect on collagen-fibronectin or polylysine substrate. In the case of polylysine, ouabain induces a 1.5-fold increase of mean Young's modulus of sensory neuron.

The next part of our investigation was dedicated to the cells of endothelium. The monolayer of the endothelial cells (ECs) forms continuous inner surface of blood vessels. The EC mechanical properties are of interest, because they are considered important for blood pressure regulation and cardiovascular disease progression. The contribution of different macromolecules and signaling events to EC mechanical phenotype is still poorly understood. Previous studies suggested the active role of actin cytoskeleton and regulatory proteins such as myosin light chain kinase in control of cellular stiffness and mechanosensing [22, 23]. According to the accomplished measurements, height distribution across EC is heterogeneous: cell center has the maximum thickness (~ 1 μm) due to the presence of nucleus, while the distal regions are significantly thinner (~ 100 nm) (Fig. 3a). Young's modulus of EC (Fig. 3b) apparently mainly reflects the nucleus mechanical properties. Probing the EC elasticity at cell periphery allows avoiding the nucleus effect. However, the cell periphery is too thin and its Young's modulus quantification could potentially be hampered by the proximity of the stiff substrate. Taking into account the typical cell indentation depth in PeakForce QNM mode (~ 100 nm), it was important to clarify whether the hard substrate would conceal the difference in mechanical properties of EC thin regions under various EC treatment conditions. In order to test this assumption, we compared the EC distal region Young's moduli of normal, latrunculin B-treated, and nocodazole-treated cells. These substances inhibit the formation of the essential components of cytoskeleton, microfilaments, and microtubules, respectively.

Our experiments showed that living mouse lung microvascular ECs grown on the gelatin substrate have large lateral dimensions and tend to form clusters. As individual ECs or cell clusters usually surpass AFM frame size, the reliable local cell height determination was problematic. Hence, we could not apply the Gavara-Chadwick correction method to derive precise Young's modulus values [24].

Young's modulus of EC periphery was analyzed within an area between cell nucleus and cell edge. It turned out that the experimental Young's modulus histogram shape best corresponded to the log-normal distribution. For this reason, we employed median Young's modulus values to characterize ECs.

The comparison of averaged median Young's modulus values of EC distal regions has led to the following results: control untreated cells exhibited the highest Young's modulus value, 140 ± 100 kPa (n = 26), whereas all inhibitors induced softening of ECs. The cells treated by latrunculin B and

nocodazole had the Young's modulus values of 60 ± 60 kPa ($n = 8$) and 70 ± 60 kPa ($n = 25$), respectively.

Statistical significance of our results was estimated using Mann–Whitney U test [25, 26]. P-values less than 0.05 were considered statistically significant. P-values were as follows: $p = 0.017$ for latrunculin B and $p = 0.003$ for nocodazole. Thus, ECs after latrunculin B and nocodazole treatment showed statistically significant change of Young's modulus.

The disassembly of microfilaments and microtubules resulted in reduction of EC periphery Young's modulus. According to our experimental data, the most drastic decrease of Young's modulus was observed in latrunculin B-treated ECs. It supports the view that actin component of cytoskeleton is the main contributor to cell elasticity [27].

Thus, our findings allow concluding that AFM indentation of thin distal regions of EC in PeakForce QNM protocol does not conceal the detection of cell stiffness alterations induced by specific inhibitors of actin and tubulin polymerization. Therefore, one can use PeakForce QNM indentation to reveal how different protein molecules affect mechanical properties of EC cortical cytoplasm.

4. Conclusion

A quasistatic AFM mode such as PeakForce QNM allows measuring the mechanical properties of living cells. Various cell types display peculiarities in mechanophenotype when subjected to external stimuli. This should be taken into account when designing high throughput AFM screening protocols of living cells for biomedical applications.

Acknowledgments

The authors are indebted to professor B.V. Krylov for his interest to our work. M.M. Khalisov and A.V. Ankudinov are grateful for the support from the Government of the Russian Federation (Grant No. 074-U01).

References

[1] Kuznetsova T G, Starodubtseva M N, Yegorenkov N I, Chizhik S A and Zhdanov R I 2007 *Micron*. **38** 824–33
[2] Efremov Yu M, Bagrov D V, Dubrovin E V, Shaitan K V and Yaminskii I V 2011 *Biofizika* **56** 288–303
[3] Gavara N 2017 *Microsc Res Tech*. **80** 75-84
[4] Rianna C and Radmacher M 2016 *AIP Conference Proceedings*. **1760** 020057-1–13
[5] Tomankova K, Kolar P, Malohlava J and Kolarova H 2012 *Current Microscopy Contributions to Advances in Science and Technology (A. Méndez-Vilas, Ed.)*. **1** 549–54
[6] Rigato A, Rico F, Eghiaian F, Piel M and Scheuring S 2015 *ACS Nano*. **9** 5846–56
[7] Calzado-Martín A, Encinar M, Tamayo J, Calleja M and San Paulo A 2016 *ACS Nano*. **10** 3365–74
[8] Nyapshaev I A, Ankudinov A V, Stovpyaga A V, Trofimova E Y and Eropkin M Y 2012 *Tech Phys*. **57** 1430–7
[9] Khalisov M M, Ankudinov A V, Penniyaynen V A, Nyapshaev I A, Kipenko A V, Timoshchuk K I, Podzorova S A and Krylov B V 2017 *Tech Phys Lett*. **43** 209–12
[10] Mozhanova A A, Nurgazizov N I and Bukharaev A A 2003 *SPM-2003. Proc. Nizhni Novgorod*. 266–7
[11] Lekka M, Fornal M, Pyka-Fosciak G, Lebed K, Wizner B, Grodzicki T and Styczen J 2005 *Biorheology*. **42** 307–17
[12] Maciaszek J L, Andemariam B and Lykotrafitis G J 2011 *J Strain Anal Eng*. **46** 368–79
[13] Rebelo L M, Sousa J S, Santiago T M and Mendes Filho J 2014 *Microscopy: advances in scientific research and education*. **1** 141–52
[14] Hategan A, Law R, Kahn S and Discher D E 2003 *Biophys J*. **85** 2746–59

[15] Khalisov M M, Timoshchuk K I, Ankudinov A V and Timoshenko T E 2017 *Tech Phys*. **62** 310–3
[16] Plakhova V, Rogachevsky I, Lopatina E, Shelykh T, Butkevich I, Mikhailenko V, Otellin V, Podzorova S and Krylov B 2014 *Act Nerv Super Rediviva*. **56** 55–64
[17] Krylov B, Rogachevsky I and Plakhova V Substance with sedative effect 2006 US 20060252824 A1
[18] Borovikova L V, Borovikov D V, Ermishkin V V and Revenko S V 1997 *Primary Sensory Neuron*. **2** 65–75
[19] Gold M S, Reichling D B, Shuster M J and Levine J D *Proc Natl AcadSci USA*. 1996 **93** 1108−12
[20] Khalisov M M, Penniyaynen V A, Esikova N A, Ankudinov A V and Krylov B V 2017 *Tech Phys Lett*. **43** 85–7
[21] Ankudinov A V, Khalisov M M, Penniyainen V A, Podzorova S A and Krylov B V 2015 *Tech Phys*. **60** 1540–4
[22] Cai S, Pestic-Dragovich L, O'Donnell M E, Wang N, Ingber D, Elson E and De Lanerolle P 1998 *Am J Physiol*. **275** 1349–56
[23] Ohlmann P, Tesse A, Loichot C, RalayRanaivo H, Roul G, Philippe C, Watterson D M, Haiech J and Andriantsitohaina R 2005 *Am J Physiol Heart Circ Physiol*. **289** 2342–9
[24] Gavara N and Chadwick RS 2012 *Nat Nanotechnol*. **7** 733–6
[25] Vargas-Pinto R, Gong H, Vahabikashi A and Johnson M 2013 *Biophys J*. **105** 300–9
[26] Jalilian I, Heu C, Cheng H, Freittag H, Desouza M, Stehn J R, Bryce N S, Whan R M, Hardeman E C, Fath T, Schevzov G and Gunning P W 2015 *PLoS One*. **10** 1–23
[27] Rotsch C and Radmacher M 2000 *Biophys J*. **78** 520–35